Compaction of thick granular layers
August 2010

J. Patrick
Opus Central Laboratories, Lower Hutt, New Zealand

Dr S. Werkmeister
University of Technology, Dresden

NZ Transport Agency research report 411

ISBN 978-0-478-36457-6 (print)
ISBN 978-0-478-36456-9 (electronic)
ISSN 1173-3756 (print)
ISSN 1173-3764 (electronic)

NZ Transport Agency
Private Bag 6995, Wellington 6141, New Zealand
Telephone 64 4 894 5400; facsimile 64 4 894 6100
research@nzta.govt.nz
www.nzta.govt.nz

Patrick, J and S Werkmeister (2010) Compaction of thick granular layers. *NZ Transport Agency research report no.411.* 40pp.

Opus Central Laboratories
P0 Box 30845
Gracefield
Lower Hutt 5040

Keywords: accelerated pavement testing, compaction, finite element modelling, granular basecourse, rutting

An important note for the reader

The NZ Transport Agency is a Crown entity established under the Land Transport Management Act 2003. The objective of the Agency is to undertake its functions in a way that contributes to an affordable, integrated, safe, responsive and sustainable land transport system. Each year, the NZ Transport Agency funds innovative and relevant research that contributes to this objective.

The views expressed in research reports are the outcomes of the independent research, and should not be regarded as being the opinion or responsibility of the NZ Transport Agency. The material contained in the reports should not be construed in any way as policy adopted by the NZ Transport Agency or indeed any agency of the NZ Government. The reports may, however, be used by NZ Government agencies as a reference in the development of policy.

While research reports are believed to be correct at the time of their preparation, the NZ Transport Agency and agents involved in its preparation and publication do not accept any liability for use of the research. People using the research, whether directly or indirectly, should apply and rely on their own skill and judgement. They should not rely on the contents of the research reports in isolation from other sources of advice and information. If necessary, they should seek appropriate legal or other expert advice.

Acknowledgements

The authors would like to acknowledge the support of David Alabaster, and the staff at the NZTA Captif facility and also David Alabaster, NZTA Captif Manager and Dr Greg Arnold of Pavespec Ltd for their peer review.

Abbreviations and acronyms

CAPTIF	Canterbury accelerated pavement testing facility
CBR	California bearing ratio
DoC	Degrees of compaction
FE	Finite element
FEM	Finite element modelling
FWD	Falling weight deflectometer
MDD	Maximum dry density
OGPA	Open-graded porous asphalt
OMC	Optimum moisture content
QA	Quality assurance
RLT	Repeat load tri-axial
SLAVE	Simulated loading and vehicle emulator
VSD	Vertical surface deformation
OGPA	Open graded porous asphalt

Contents

Executive summary

The majority of pavements in New Zealand consist of a granular base with a chipseal surfacing. The specifications for constructing these pavements call for the compaction level to be closely controlled and monitored using nuclear density meters.

There have been a number of high-profile early failures in New Zealand (rut depths greater than 20mm observed early in the pavement life) associated with 'greenfield' pavements (pavements not subjected to traffic during construction) where the granular layers were greater than approximately 400mm thick. It is uncertain if the rutting was due to poor construction control, difficulties in measuring the density of thick layers with a meter operating in backscatter mode, or because of a lack of traffic on the pavement. In response, a research project was initiated at the NZ Transport Agency's accelerated pavement testing facility (CAPTIF) to investigate the effect of constructing the basecourse and sub-base to a range of densities (88% to 95% of maximum dry density (MDD).

In addition to the CAPTIF trial a more theoretical analysis consisting of comparing the theoretical stress and strain distribution under a vibratory roller and a standard heavy vehicle was performed.

The conclusion of the research was that in using conventional New Zealand construction techniques and specifications, some post construction deformation of greenfield pavements appeared to be inevitable. The permanent strain developed manifested itself into a larger rut depth as the granular thickness increased. However, the rut depth should not approach the levels (20mm) that prompted the initiation of this research.

This research demonstrated that the initial post construction deformation of a thin-surfaced granular pavement was affected by the compaction level achieved in the field although the depth of the rut would be relatively small. It also demonstrated that there was probably a contribution from the compaction equipment used.

The results of the repeat load tri-axial (RLT) testing and finite element modelling (FEM) supported the above conclusions in that a degree of compaction of 88% MDD would not result in significant rutting in the pavement. The results suggested that after one million load applications the difference in rut depth of a granular layer of 450mm depth that had been compacted to 88% MDD and one that had been compacted to 95% MDD would be approximately 3mm.

The results of the finite element (FE) calculations indicated that the maximum vertical elastic strains and vertical compressive stress induced by a 3t-roller drum (high amplitude dynamic load + static drum weight) in the upper part of the basecourse were smaller compared with the stresses and elastic strains induced by a 40kN dual wheel for the pavements investigated. The vertical compressive stress and elastic strains induced by a 3t-roller drum at the lower part of the basecourse were considerably higher than the stress and strains induced by a 40kN loaded dual wheel for the pavements investigated.

As the compaction system did not build up residual stresses in the pavement, when traffic loading occurred, granular material was moved causing the build up of stresses that could resist the wheel loading.

The shear deformation found in the field was associated not just with post-construction rutting but was exacerbated by water being forced through the surface under traffic tyre forces.

Research into the influence of the compaction methodology and the waterproofing ability of thin surfacings on the performance of unbound granular materials is continuing.

Abstract

There have been a number of high-profile early failures in New Zealand pavements (rut depths greater than 20mm observed early in the pavement life) associated with 'greenfield' pavements (pavements not subjected to traffic during construction). It is uncertain if the rutting was due to poor construction control, difficulties of measuring density of thick layers or a function of lack of traffic on the pavement. In response, a research project was initiated to investigate in the NZ Transport Agency's accelerated pavement testing facility (CAPTIF) the effect of constructing the basecourse and sub-base to a range of densities (88% to 95% of maximum dry density).

In addition to the CAPTIF trial a more theoretical analysis consisting of comparing the theoretical stress and strain distribution under a vibratory roller and a standard heavy vehicle was performed.

The conclusion of the research was that by using conventional New Zealand construction techniques and specifications some post-construction deformation of greenfield pavements appears to be inevitable. The permanent strain developed will manifest itself into a larger rut depth as the granular thickness increases. However, the rut depth should not approach the levels (20mm) that prompted the initiation of this research.

1 Introduction

The majority of pavements in New Zealand consist of a granular base with a chipseal surfacing. In construction of these pavements the specifications call for the compaction level to be closely controlled and monitored using nuclear density meters.

There have been a number of high-profile early failures in New Zealand (rut depths greater than 20mm observed early in the pavement life) associated with ‘greenfield’ pavements (pavements not subjected to traffic during construction) where the granular layers were greater than approximately 400mm thick. It is uncertain if the rutting was due to poor construction control, difficulties in measuring density of thick layers with a meter operating in backscatter mode, or because of a lack of traffic on the pavement. In response, a research project was initiated at the NZ Transport Agency's (NZTA) accelerated pavement testing facility (CAPTIF) to investigate the effect of constructing the basecourse and sub-base to a range of densities (88% to 95% of maximum dry density (MDD)).

In addition to the CAPTIF trial a more fundamental analysis consisting of comparing the theoretical stress and strain distribution under a vibratory roller and a standard heavy vehicle was performed.

This report presents the results of the investigations and gives conclusions and recommendations for further research.

2 Compaction specification

Specification B/2 for the construction of unbound granular pavement layers (TNZ 2005) sets out the requirements for compaction of the granular sub-base and basecourse layers. It allows the development of a 'plateau density' which is the maximum density the layer reaches under controlled rolling trials. The acceptance criteria of pavement layers other than those where a plateau density has been established is based on achieving a minimum compaction level in terms of percentage of MDD. MDD is determined in the laboratory using a vibratory hammer compaction method. See New Zealand Standard 4402:1986 tests 4.1.3.

The wording of the specification is reproduced below:

> *7.6 Acceptance Criteria for pavement layer compaction*
>
> *The pavement layer shall be compacted to a uniform, dense, stable condition.*
>
> *Compaction testing of the pavement layers shall be carried out in lots. A lot is defined as a section where the pavement layer appears homogeneous and evenly compacted. The area of a lot shall not exceed 1000 m^2.*
>
> *The degree of compaction for each lot shall be determined by testing at least five randomly selected areas. The compaction requirements shall be met if the mean and minimum compaction values of the tests taken comply with the values in Figure 2. In preference to random selection the Engineer may carry out any testing for uniformity to determine the location of density tests. The Maximum Dry Density shall be determined for each layer at minimum frequency of one Maximum Dry Density per 5,000m2 of material laid. If the aggregate source, face at the source, or processing method is changed then a new Maximum Dry Density shall be determined and the Engineer informed.*

The minimum density requirements are given in table 2.1. In addition, the granular layers must be less than 80% saturation before a surfacing is applied.

Table 2.1 Mean and minimum value of pavement layer compaction as percentage of maximum dry density specified in TNZ specification B/2

Value	Sub-base	Basecourse
Mean	≥95%	≥98%
Minimum	≥92%	≥95%

Advice on appropriate compaction plant is given in the notes to B/2 and is reproduced below:

> *TNZ B/2 1994 provided guidance on appropriate levels of compaction by specifying parameters for the rollers to be used and this information may still be useful where difficulties are encountered reaching the requirements of TNZ B/2 2004. It should also be noted that the OWC for the roller will most likely be dryer than the laboratory test. TNZ B/2 1994 noted that compaction shall be achieved by the minimum necessary number of passes of compaction plant, and compaction plant shall include type (i) for primary compaction, and may include either or both types (ii) and (iii) for the final consolidation of the surface*
>
> *(a) Type (i): Vibratory roller of either double or single vibrating drum of not more than 3.2 tonnes mass per metre of roll width having vibration frequency of not less than 2200 vpm (37 Hz).*

Vibrating rollers not exceeding the above weight limit but of frequency less than 2200 vpm (37 Hz) are approved providing the nominal amplitude does not exceed that shown relative to the weight in tonnes per metre of roll width in Figure 1.

Vibrating rollers of less than 1 tonne per metre of roll width shall not be used to compact any pavement layer of more than 175 mm uncompacted thickness.

(b) Type (ii): Any non-vibrating smooth, steel-tyres roller having not less than 1 tonne nor more than 3.2 tonnes mass per metre of roll width.

(c) Type (iii): Pneumatic tyred roller having a minimum weight when operating of not less than 7 tonnes, spread over at least seven rubber tyred pneumatic wheels.

The compaction levels specified were based on research performed in 1995 (Patrick and Alabaster 1998). In the research the density of granular pavements that had been subjected to three months of traffic on state highways was compared with the laboratory-determined MDD. The five pavements analysed had all settled at approximately 95% of the MDD.

3 Field experience

A summary of the details of three New Zealand pavements that rutted early in their lives is given in table 3.1.

Each pavement was on a state highway and constructed to the TNZ B/2 specification. The base-course materials all complied with the TNZ M/4 specification which specifies a 40mm maximum particle size, low to zero plasticity and at least 70% broken faces in the coarse aggregate. The sub-base materials were all a 65mm maximum particle size partly to fully crushed.

The rut depths given in table 3.1 were measured on the sites within six months of opening to traffic. On each site the pavement construction was completed before it was opened to traffic.

A review of the construction quality records and post-mortem testing found that all sites complied with the specification requirements.

Table 3.1 Details of three premature rutting failure sites

	Site 1	Site 2	Site 3
Surfacing	30 OGPA	30 OGPA	Chipseal
Basecourse	150	180	150
Sub-base	450	390	200
Vehicles/lane/day	9000	5000	6000
Rut depth at 6 months	20	20	15
Approx ESA at 6mths	2.3×10^5	1.2×10^5	1.3×10^5

3.1 Site 1

This is a site near Wellington where the state highway was widened to accommodate another lane.

A comparison of the density tests in the trenches was made to the quality control test results supplied by the contractor during construction. The results are summarised in table 3.2 for base course and table 3.3 for sub-base. The maximum dry densities of 2270 and 2230kg/m3 for the basecourse and sub-base respectively were taken from the test results supplied by the contractor. In the investigations the density was determined using the backscatter and direct transmission modes from the base course and direct transmission mode only for the sub-base. The concern was that the removal of the surfacing and granular layers could disturb the underlying material and give an incorrect reading with the densometer. It was considered that the direct transmission mode would minimise the effect of any surface disturbance.

Table 3.2 Basecourse densities from the contractor and investigations

	Contractor Q/A	Trench investigation	
		Back Scatter	150mm
Average	2281	2170	2235
% 0f MDD	100.5	95.6	98.5
SD	13.8	51.1	89.7
N	8	3	5

Table 3.3 Sub-base density comparison from the contractor and the trench investigations

	Contractor	Trench investigation
		Average of 150mm and 300mm
Average	2214	2051
% of MDD	99.3	92.0
SD	20.3	134.4
n	10	5

The conclusions from the investigations were:

1 Both the contractor's test results and the trench tests indicated that the compaction level for the basecourse was approximately 98%. For the rutting to have occurred in the basecourse the 150mm layer would have needed to compact by 20mm (to form the rut) which would be the equivalent of a change in density of 13% (20/150). This implied that for the deformation to have occurred in the basecourse the density at construction would have needed to be 82% MDD (98% -13%). Such a low level of compaction would have resulted in a very loose material that could not be sealed.

2 For the sub-base, using the above argument, the change in the percentage of compaction of a 450mm layer to result in a 20mm rut would be 4%. The test results from the trenches indicated a compaction level of 92% and one site with a low density of 1816 kg/m^3. In contrast to the basecourse results the contractor's test results and the trench results did not coincide. A sub-base compaction level of 88% MDD would again have been very noticeable and was considered unlikely.

3.2 Site 2

On this site a four-lane pavement was constructed from granular base layers surfaced with a chipseal and then an open-graded porous asphalt (OGPA). Soon after opening rutting occurred that cracked the OGPA and water entered the pavement leading to shear of the basecourse.

An extensive investigation reviewed the pavement design, drainage performance and construction records. Test pits were dug and the properties of the materials were confirmed. A falling weight deflectometer (FWD) survey was also performed and the results analysed to confirm the material properties.

The conclusion of the investigation was that post-construction densification occurred in the basecourse and to a small extent in the sub-base layers. This occurred even though the density of the basecourse and sub-base met the contract requirements. A plot of the densities achieved on part of the project is given in figure 3.1.

Figure 3.1 Basecourse densities from construction records on site 2

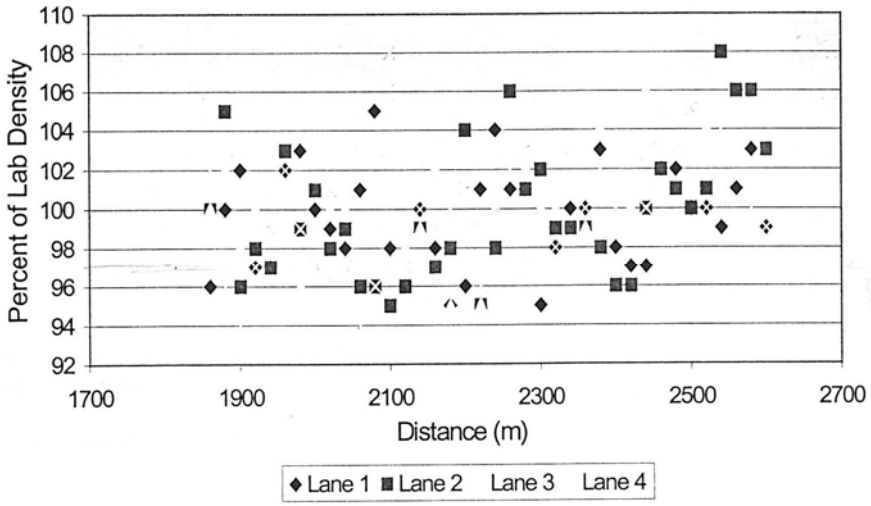

3.3 Site 3

On this site a second lane was constructed on both sides of an existing two-lane section of state highway. The passing lane was completed in February 2006. A step at the interface was noted after the pavement had been sealed which resulted in a step up from the new pavement to the old.

Within a few weeks of construction the presence of a rut was noted in the right-hand wheelpath.

The transition is generally parallel to the lane markings, except at the beginning and end. The photos below show the relativity of rut and transition, as constructed.

Figure 3.2 Trenched profile (left) and rutting under straight edge (right)

The outer wheelpath is indicated by the track in the surface (figure 3.2 left photo) and by the left end of the bar resting on the road surface (figure 3.2 right photo).

It was originally thought that the resulting rut depth was as deep as 40mm, but this depended on the data used. When recognition of the change in crossfall within the existing pavement was made, the consultant proposed that the rut depth was less than half this figure.

Figure 3.3 Cross-section profile

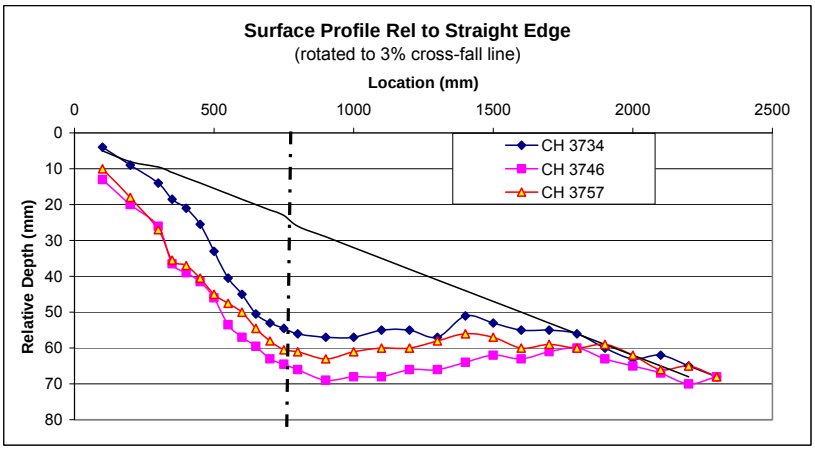

Construction and quality assurance (QA) processes appeared to have been satisfactory.

The pavement structure, as measured by the FWD, appeared to be satisfactory

4 CAPTIF testing

4.1 Description

NZTA's accelerated pavement testing facility (CAPTIF) was used to explore the effect of the compaction level on the subsequent granular base-course behaviour. Details of the test track can be found in Pidwerbesky (1995).

CAPTIF is located in Christchurch, New Zealand. It consists of a 58m long (on the centreline) circular track contained within a 1.5m deep x 4m wide concrete tank so that the moisture content of the pavement materials can be controlled and the boundary conditions are known. A centre platform carries the machinery and electronics needed to drive the system. Mounted on this platform is a sliding frame that can move horizontally by 1m. This radial movement enables the wheel paths to be varied laterally and can be used to have the two 'vehicles' operating in independent wheel paths.

At the ends of this frame, two radial arms connect to the simulated loading and vehicle emulator (SLAVE) units. These arms are hinged in the vertical plane so that the SLAVEs can be removed from the track during pavement construction, profile measurement, etc and in the horizontal plane to allow vehicle bounce. Full details can be found in Pidwerbesky (1995); it basically consists of two wheel assemblies that can each apply a dual-tyred half-axle load of 40kN.

For this research three sections were constructed on a prepared subgrade with a California bearing ratio CBR of 3. The pavement consisted of 450mm of a 40mm maximum particle size basecourse, which in complying with the TNZ M/4 specification would be regarded as a premium material. The intention was to construct three sections to 85%, 90% and 95% of MDD.

The 450mm basecourse layer was constructed in three 150mm lifts which were compacted using a vibratory plate compactor. Due to the relatively tight radius of the test track it is very difficult to use a full-sized vibratory roller and the plate compactor is the usual compaction system used.

It was found impossible to construct each layer to the specific density. This was especially noticeable with the target of 85% of MDD. After spreading and lightly compacting the layer, the percentage of MDD was over 88%. The average compaction level obtained on each layer is given in table 4.1.

Table 4.1 Basecourse densities as % of MDD

Depth from subgrade	Site 1	Site 2	Site 3
0–150mm	88.0	95.0	98.4
150–300	89.0	93.2	97.3
300–450	93.8	94.4	94.3
Average	90.6	94.2	96.7

The three sections are referred to in this report as 88% of MDD, 95% of MDD and 98% of MDD reflecting the compaction level achieved on the first (bottom) layer.

The final surfacing was a 25mm layer of dense graded asphaltic concrete.

The pavement was then loaded and a transverse profile measured at regular intervals. For each section at nine cross sections the vertical surface deformation (VSD) was measured at 25mm intervals.

4.2 Vertical surface deformation

The VSD is more conveniently measured at CAPTIF with the transverse profilometer than rut depth under a straight edge. VSD is defined as the vertical difference between the start reference level of the pavement and that measured. VSD and rut depth are very similar where there is no lateral heave of the pavement. In the 88% of MDD section an area of rutting of 16 to 18mm developed at 186,000 load cycles and the section was then resurfaced.

The average difference of VSD at 187,000 cycles and after resurfacing was used to apply a correction to the measurements so that the trend in VSD could be determined.

Figure 4.1 shows the relationship between the average of the nine VSD measurements on each section with loading cycles It can be seen that the 95% of MDD and 98% of MDD are nearly identical but the 88% of MDD has a higher level of deformation. The resurfacing at 186,000 cycles appears to have had a significant effect on the trends especially the 88% MDD.

Figure 4.1 Number of load cycles versus VSD for the test pavements

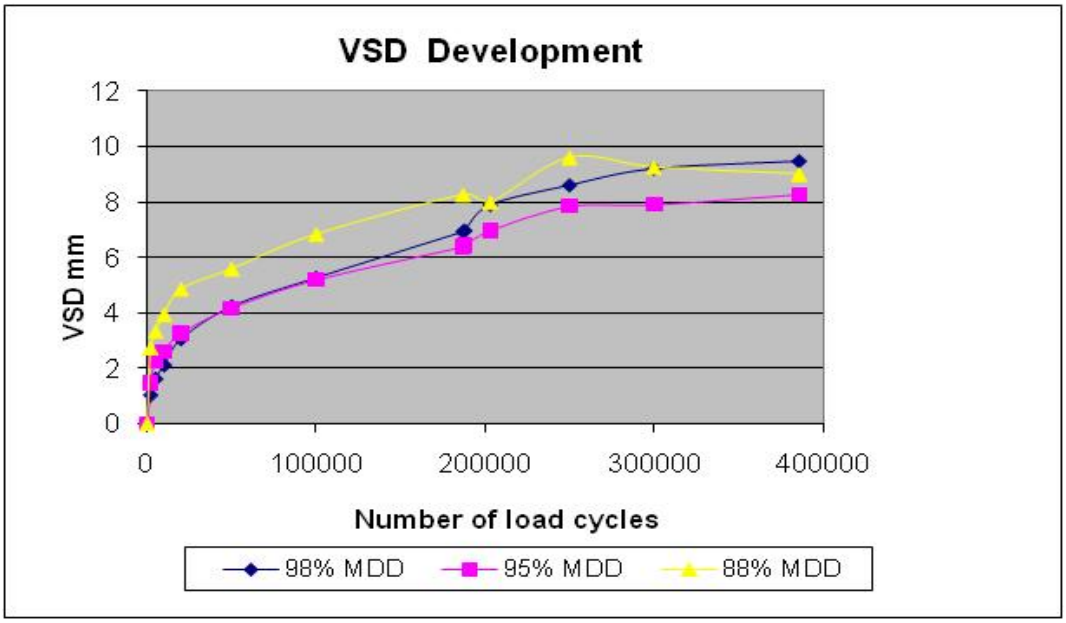

An examination of the data up to the 187,000 cycles together with error bands representing a plus and minus one standard deviation range is shown in figure 4.2. In the figure it can be seen that most of the difference between the 88% of MDD and the other two sites occurs in the first 20,000 load cycles.

Figure 4.2 Number of load cycles versus VSD for the test pavements up to 186,000 cycles

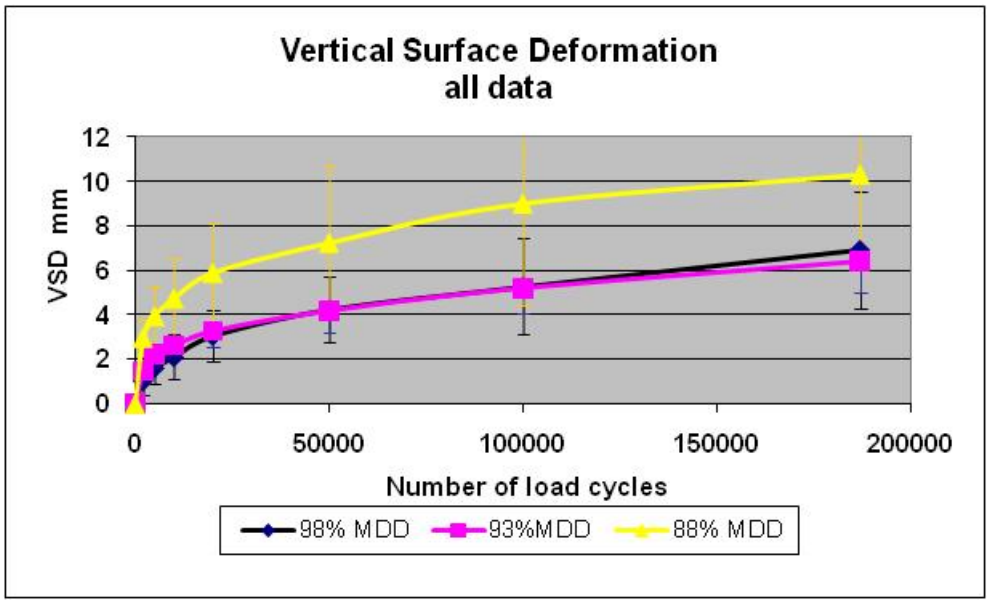

The failure in the 88% MDD section occurred at adjacent stations and the data with these two stations plotted separately is shown in figure 4.3. The dramatic failure is evident. It appears there was significant deformation occurring in stations 25 and 26 during the first 20,000 cycles. When this data was removed the other seven cross-sections compared well with the higher compaction level data.

Figure 4.3 Vertical surface deformation

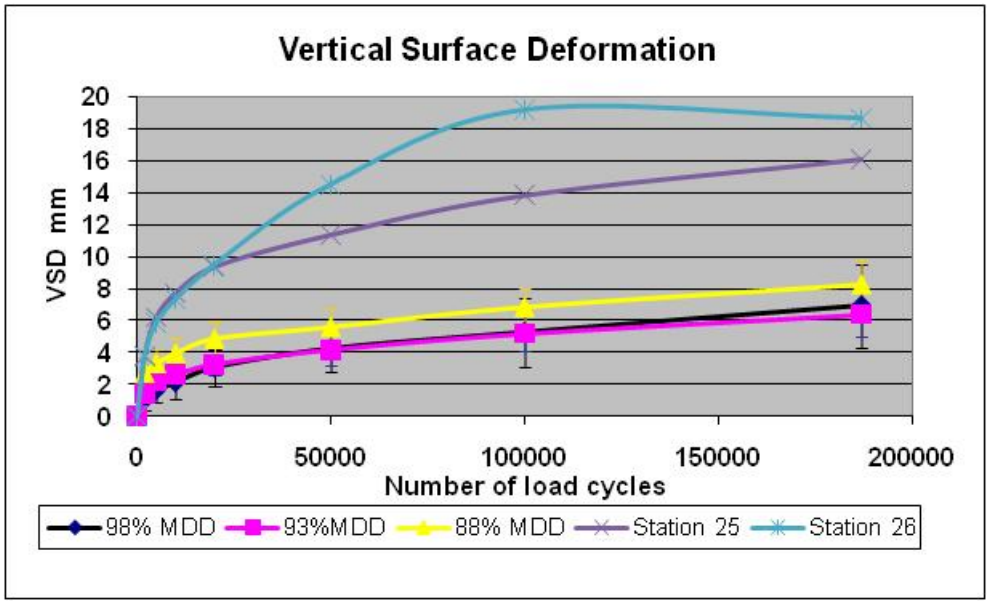

4.3 Densities

The densities of the layers were measured at construction and again after the termination of the loading. The MDD from the vibratory hammer test was 2260kg/m^3.

The average densities are given in table 4.2.

The densities of the layers before construction and after trafficking are given in table 4.3. The densities were not measured after the failure on the 88% MDD section.

As there was concern over the disturbance to the material when removing the layers, density tests after trafficking were measured in direct transmission mode (depth of probe 150mm) as well as back scatter mode at the same locations. In table 4.2 the results are presented in terms of percentage of the MDD.

Table 4.2 Before and after densities of the sections and layers

			88% MDD	93% MDD		95% MDD	
			BS	BS	DT	BS	DT
BC1`	As laid	mean	2000	2154		2224	
		Sd	59	87		32	
		No tests	12	10		9	
	After	mean		1739	1907	1879	2026
		Sd		143	77	192	122
		No tests		16	16	9	9
BC2	As laid	mean	2008	2107		2199	
		Sd	59	35		47	
		No tests	8	6		6	
	After	mean		1810	2007	2147	2168
		Sd		178	65	36	44
		No tests		16	16	9	9
BC3	As laid	mean	2120	2133		2132	
		Sd	34	34		21	
		No tests	16	12		16	
	After	mean		1930	1927	1902	2014
		Sd		69	100	98	55
		No tests		17	17	9	9

Table 4.3 Before and after percentage of MDD for sections and layers

			88% MDD	93% MDD		95% MDD	
			BS	BS	DT	BS	DT
BC1`	As laid	mean	88.5%	95.3%		98.4%	
		Sd	2.6%	3.9%		1.4%	
		No tests	12	10			
	After	mean		76.9%	84.4%	83.2%	89.6%
		Sd		6.3%	3.4%	8.5%	5.4%
		No tests		16	16	9	9
BC2	As laid	mean	88.8%	93.2%		97.3%	
		Sd	2.6%	1.5%		2.1%	
		No tests	8	6		6	
	After	mean		80.1%	88.8%	95.0%	95.9%
		Sd		7.9%	2.9%	1.6%	2.0%
		No tests		16	16	9	9
BC3	As Laid	mean	93.8%	94.4%		94.3%	
		Sd	1.5%	1.5%		0.9%	
		No tests	16	12		16	
	After	mean		85.4%	85.3%	84.2%	89.1%
		Sd		3.0%	4.4%	4.3%	2.4%
		No tests		17	17	9	9

The data suggests that the density decreased during the trafficking and this occurred on all layers.

4.4 Stations 26 and 27

Stations 26 and 27 are the locations where the rapid failure occurred.

The density data for the 88% MDD section is shown in figure 4.4. In figure 4.4, BC1 refers to the bottom layer and BC2 and BC3 refer to the subsequent layers. Although station 27 has a low density in BC1 so does station 31 which did not suffer premature failure.

Figure 4.4 As constructed densities of the 88% MDD section

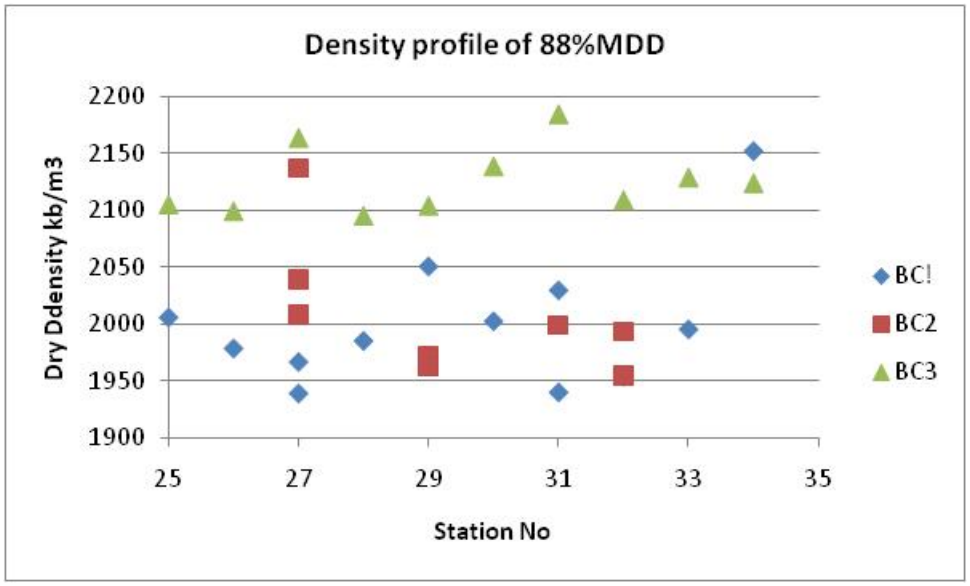

5 Finite element modelling

For a detailed investigation of pavement stress and strains, a three-dimensional computational model is required. ReFEM, a FE program was used to carry out this investigation. A rectangular model was developed to simulate the pavement. By making use of symmetry (quarter model) in the geometry the computational effort was reduced. The length of the FE section was 2.4m (2 x 1.2m) and the width of the section was 4.0m (2 x 2.0m). Table 5.1 shows the granular pavements investigated within this research.

Table 5.1 Granular pavements investigated

Pavement	Thickness of the granular layer [mm]	Number of the elements in vertical direction of the basecourse layer [-]	Thickness of the subgrade [mm]
1	200	4	1200
2	300	4	1200
3	500	10	1200
CAPTIF	450	9/10	1050

The subgrade was modelled by two (loaded by a roller drum, each element 600mm high) or four elements (loaded by a tyre, each element 300mm high) according to table 5.1. Figures 5.1 and 5.2 show the FE meshes for a pavement with a 200mm thick basecourse layer.

The basecourse was modelled by four or 10 elements according to table 5.1. The asphalt layer was modelled by two elements, each 12.5mm high (for the pavements loaded by a wheel). The mesh used in the analysis was finest at the contact zone (element size – 66.6mm x 66.6mm x height) where large stress and strain gradients were expected. The bottom of the subgrade was prevented from axial movement in the three directions.

Figure 5.1 FE mesh for a pavement with a 200mm thick basecourse and loaded by a 3t-roller drum

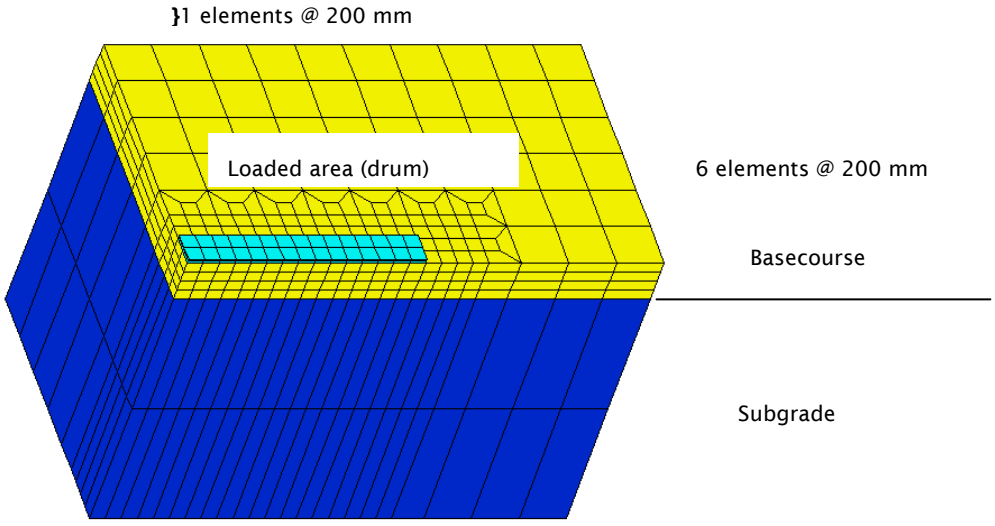

Figure 5.2 FE mesh for a pavement with a 400mm thick basecourse and loaded by a 40KN dual wheel

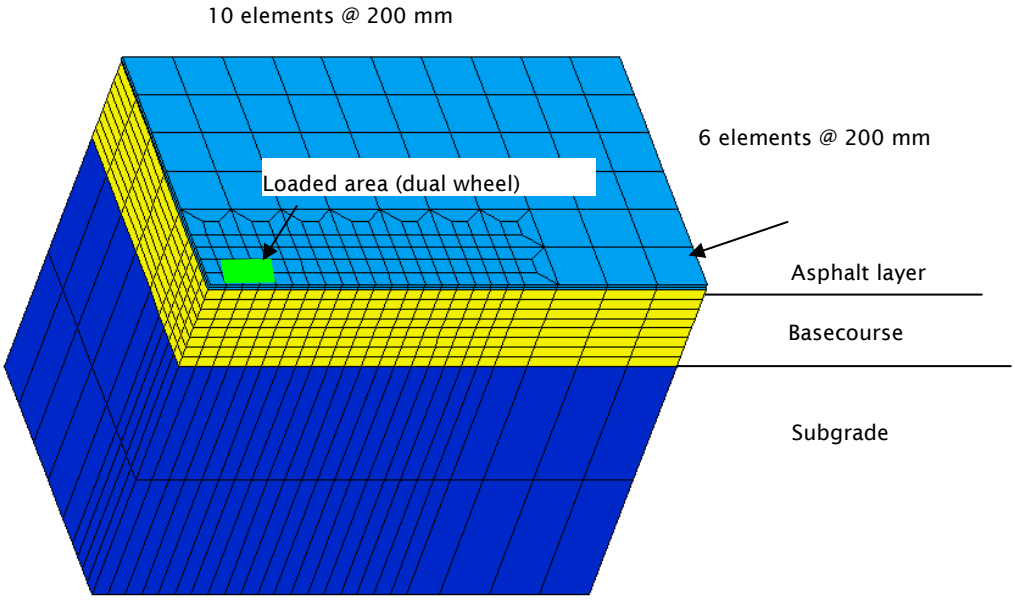

5.1 Dual wheel

In order to determine the contact area of the tyre for use in the pavement modelling stage of this research, the tyre footprints measured at CAPTIF under a 40kN loaded dual wheel were used. The dimension of the tyre footprint was approximately rectangular, 230mm long and 215mm wide (each wheel) when loaded to 40kN The loaded area was 0.0495m2 (each wheel). However, this area could not be modelled identically in the FE program used in this analysis. The loaded area of the truck was composed of 3 by 2 x 2 elements (each wheel 0.0533m2) as shown in figure 5.2. The contact pressure of 0.338 N/mm2 was assumed to be uniformly distributed over the contact area.

5.2 Roller drum

Vibratory rollers have been used for many years in pavement construction. The drums are smooth for compaction of granular basecourse layers. The optimum design of a vibratory roller is difficult. The roller should compact efficiently on different types of materials and in different stages from loose to fully compacted. It is well known that bouncing on the layer surface can enter undesirable vibration states like double jump and rocking motion. Existing rollers have normally one or two different amplitude settings (see table 5.1) and therefore represent a compromise regarding efficient compaction under various soil and basecourse conditions.

A system consisting of a vibratory roller compacting a basecourse layer is very complex. The FE model has to be simplified in many respects and focused on the parameters that are most important for the problem at hand. The modelling of the different details of the roller may be important for the roller designer; however, within this analysis the pavement structure was modelled in detail and as accurately as possible.

A smooth drum roller, type Caterpillar CS 563C, was selected to calculate the load under a typical 3t-vibratory roller drum used for basecourse compaction. The width of the contact area is dependent on the soil/basecourse stiffness and was assumed to have a length of 266mm for a high amplitude dynamic load

and with a width of 133mm for a low amplitude dynamic load (Hamm, pers comm 2007). The roller specification is listed in table 5.2. The mass per unit length is 1.4t/m which is inside the range of 1-3.2 t/m recommended in the NZTA B/2 notes.

Table 5.2 Roller specification (Ping et al 2002)

Roller type		Caterpillar CS 563C
Drum diameter	[mm]	1524
Drum width	[mm]	2,100
Drum module weight (static load)	[t]	2.96
High amplitude dynamic load	[t]	15.195
Loaded area – High amplitude dynamic load	[m^2]	0.532
Low amplitude dynamic load	[t]	4.65
Loaded area – Low amplitude dynamic load	[m^2]	0.266

The loaded area of the roller drum was composed of 15 by 2 x 2 elements for a high-amplitude dynamic load (loading area 0.532m2 – 266mm x 2000mm) as shown in figure 5.1 and of 15 by 1 x 2 elements for a low-amplitude load (loading area 0.266m2 – 133mm x 2000mm). Because of the high stiffness of the roller drum it is assumed that the roller drum does not deform significantly in transversal and vertical direction during the compaction process. Hence, the roller drum was modelled as a rigid plate with an E-value of 320,000N/mm2 in transversal and vertical direction.

The elastic deformation of the basecourse/subgrade is assumed to be governed by a parabolic load (Sandström 2006) shown in figure 5.3.

Figure 5.3 Assumed vertical stress distribution under a roller drum

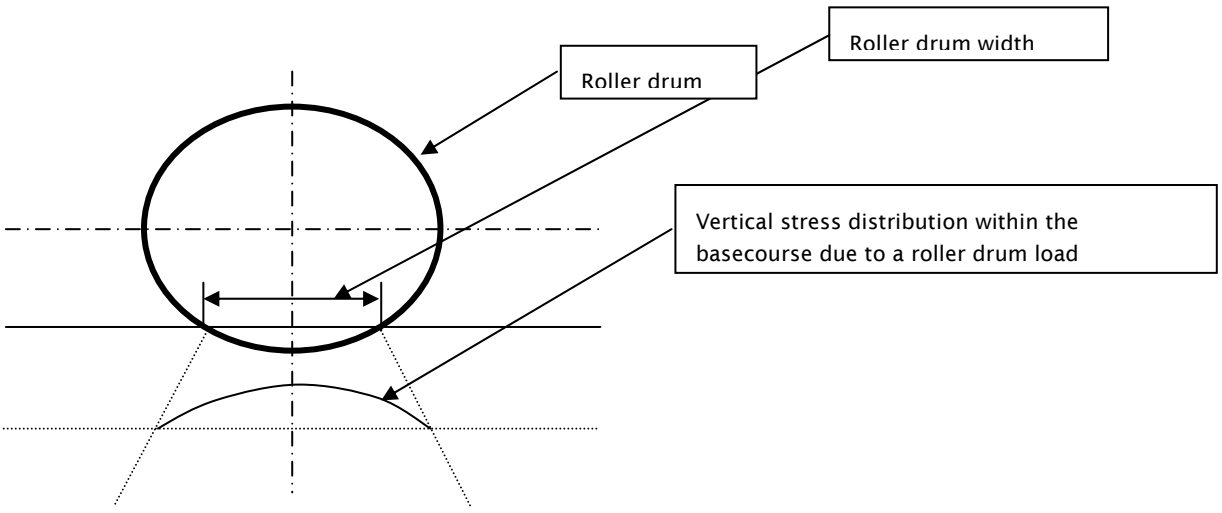

In order to reproduce this parabolic load, the roller drum was modelled with a very low E-modulus value of 50N/mm2 in longitudinal direction. Calculations were made of the peak stresses and vertical elastic strains within the pavement due to high-amplitude and low-amplitude vibratory compaction load at conventional travel speed (4.4 to 6.6km/h).

5.3 Material models

5.3.1 Asphalt

The asphalt layer was treated as linearly elastic (□ = 0.35). An E-value of 3,000N/mm2 was assumed.

5.3.2 Basecourse

In order to determine the parameter for the elastic and plastic model, repeat load tri-axial (RLT) tests were conducted on the basecourse material used at CAPTIF. Resilient modulus tests as well as permanent strain tests according to the draft NZTA RLT Standard T15 were conducted at two different degrees of compaction (DoC) (87% and 95%) and at a moisture content of 70% of the optimum moisture content (OMC).

5.3.2.1 Nonlinear Dresden Model for the basecourse

On the basis of RLT testing an empirical non-linear elastic-plastic deformation design model (Dresden Model) was formulated. This model has been implemented into the FE program. In this section only a short overview on the modelling is given. Further details are available elsewhere (Werkmeister 2003; Oeser 2004). This non-linear elastic model is expressed in terms of modulus of elasticity E and Poisson's ratio □ as follows:

$$E = p_a \left(Q + C \cdot \left(\frac{\sigma_3}{p_a} \right)^{Q_1} \right) \cdot \left(\frac{\sigma_1}{p_a} \right)^{Q_2} + D \qquad \text{Equation 5.1}$$

$$\nu = R \cdot \frac{\sigma_1}{\sigma_3} + A \cdot \frac{\sigma_1}{p_a} + B \quad (2)$$

where σ_3 [kPa] minor principal stress (absolute value); σ_1 [kPa] major principal stress (absolute value); D [kPa] constant term of modulus of elasticity; Q, C, Q1, Q2, R, A, B model parameters. On the basis of the results of multi-stage RLT tests it is possible to determine the parameters of the elastic model. Table 5.3 shows the parameters for the Dresden Model used for the FE calculation process.

Table 5.3 Parameter for the elastic Dresden-Model

Parameter	Unit	95% MDD	88% MDD
Q	[-]	14,004	14,003
C	[-]	6540	1227
Q_1	[-]	0.346	0.555
Q_2	[-]	0.333	0.333
D	[kPa]	65,000	65,000
R	[-]	0.056	0.056
A	[-]	-0.0006	-0.0006
B	[-]	0.483	0.483
		1	1
p_a	[kPa		

5.3.3 Subgrade

To overcome the limitation of the depth of the FE model the subgrade was modelled as a linearly elastic material with an E-value of 70N/mm2 and a □-value of 0.4 (pavements 1 to 3).

For the CAPTIF pavement, the subgrade was modelled as a linearly elastic material with an E-value of 30N/mm2 and a □-value of 0.4 because a CBR value of 3 was measured at the subgrade at CAPTIF.

5.4 Results

5.4.1 Stress distribution (high amplitude dynamic load + static drum weight)

Figure 5.4 shows the pattern of vertical compressive stress developed in the pavement structure when a 40kN loaded dual wheel and a 3t-roller drum (high amplitude dynamic load + static drum weight) travels over the pavement layers.

Figure 5.4 Vertical compressive stress distribution under a 40kN loaded dual wheel (left) and under a 3-t roller drum (right) within a granular pavement with a 200mm thick basecourse (DoC 95%)

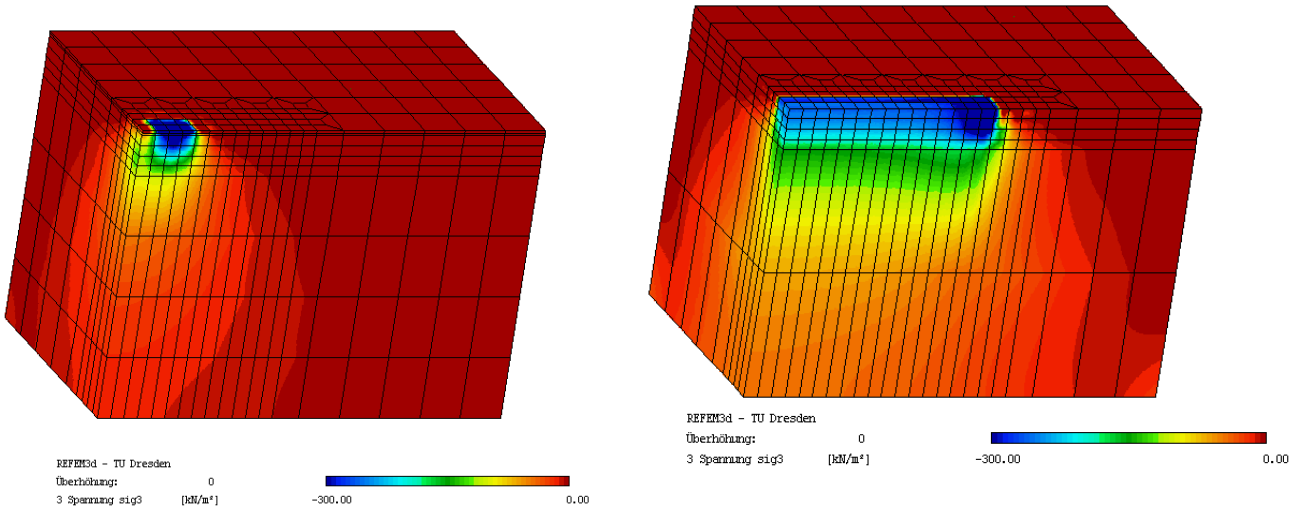

The maximum compressive stress under a dual wheel naturally occurs in the middle of the wheel path next to the surface. It is clear that the top layers (here mainly the basecourse) are vitally important to meet induced strains causing premature failure and should be compacted sufficiently. Furthermore, the results of the FE calculation illustrate that the highest vertical stress under a rigid 3t-steel roller drum occurs next to the drum edges. Figure 5.5 shows the vertical stress distribution under the drum centre, the drum edge, the dual wheels and between the dual wheels.

Figure 5.5 Vertical compressive stress under a 3t-roller drum and a 40kN loaded dual wheel, basecourse thickness 200mm (DoC 95%), high-amplitude dynamic load + static drum weight

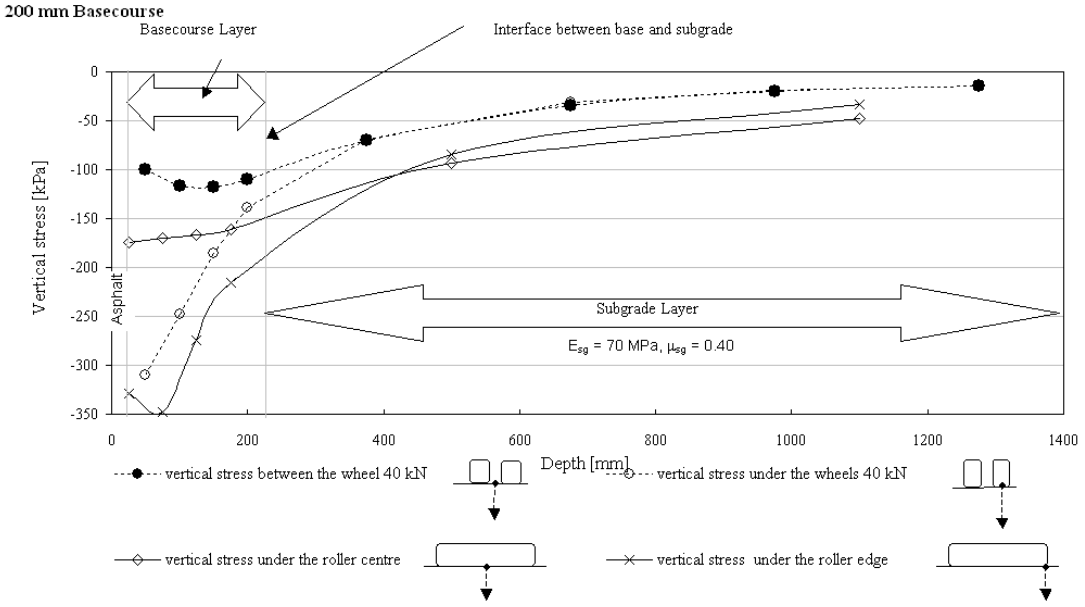

The stress values shown in figure 5.5 demonstrate that the vertical stress in the upper two-thirds of the basecourse under a 40kN wheel load is significantly higher compared with the vertical stress under a 3t-roller drum (drum centre; high-amplitude dynamic load + static drum weight). Only the vertical stress under the roller drum edge is higher compared with the stress under a 40kN loaded dual wheel. The vertical compressive stress induced by a 3t-roller drum at a pavement depth of 175mm and deeper is considerably higher than the vertical stress induced by a 40kN loaded dual wheel. It can be concluded that the roller drum induces higher stress in the subgrade when compacting a 200mm thick basecourse layer compared with the stress induced by a 40kN loaded wheel load. Hence, this roller should be able to apply sufficient compaction effort on the lower part of the basecourse and the subgrade only.

5.4.2 Strain distribution (high amplitude dynamic load + static drum weight)

The vertical elastic strains determined under a 40kN loaded dual wheel and under a 3t-roller drum (high-amplitude dynamic load + static drum weight) are shown in figure 5.6.

Figure 5.6 Comparison of vertical elastic strains under a 3t-roller drum and a 40kN loaded dual wheel, 200mm basecourse (DoC 95%); high amplitude dynamic load + static drum weight

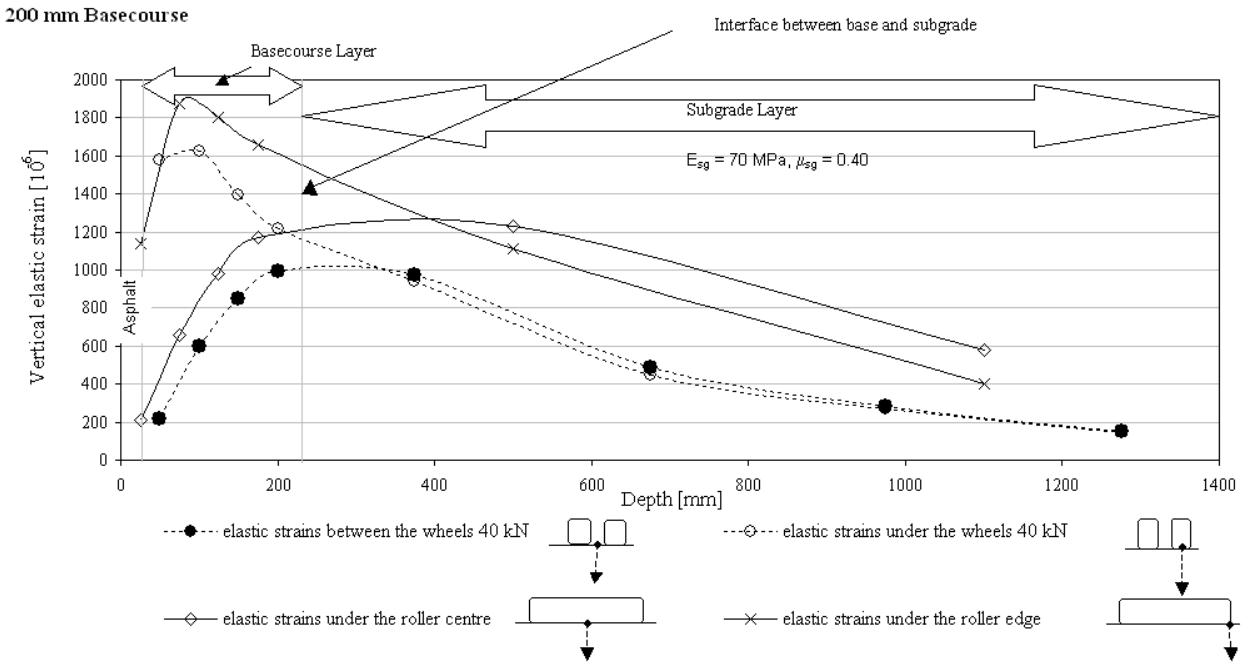

Figure 5.7 illustrates that the vertical elastic strains in the basecourse under a 40kN loaded dual wheel are significantly higher compared to the vertical elastic strains induced by a 3t-vibratory roller drum (roller drum centre). However, under the edge of the roller drum higher vertical elastic strains are induced in the pavement compared with the 40kN loaded dual wheel. In addition, the vertical elastic strains occurring under a 3t-roller drum (drum centre) in the subgrade are on average twice as high as the strains occurring under a 40kN loaded dual wheel.

Figure 5.7 Vertical strains under a roller drum and under a 40kN loaded dual wheel within a granular pavement with a 200mm thick basecourse (DoC 95%); high amplitude dynamic load + static drum weight

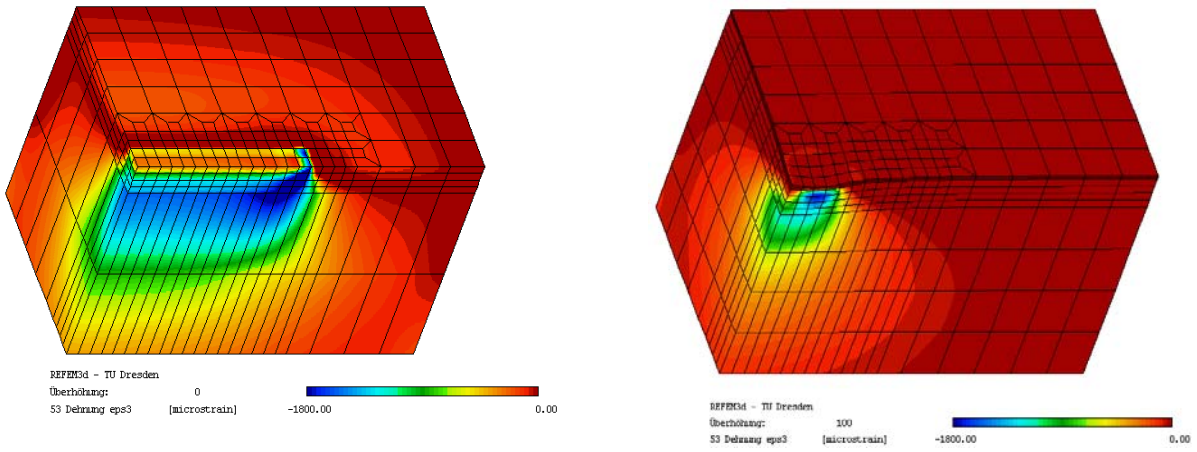

Furthermore, figure 5.8 clearly illustrates that the highest vertical elastic stains due to a 3t-roller drum (drum centre) appear in the subgrade. In contrast, the highest stains due to a 40kN loaded dual wheel can be observed in the basecourse.

5.4.3 Strain distribution (low amplitude dynamic load + static drum weight)

Because of the lower dynamic load at low amplitude settings (table 3.1) the sinking of the roller drum into the pavement surface is much smaller compared with the high-amplitude settings. Hence, at low-amplitude settings of the roller the biggest drum contact area is significantly smaller compared with the contact area of the drum at high-amplitude settings.

The results of the FE calculations demonstrate (figure 5.3) that the vertical elastic strains due to a 3t-roller drum (drum centre; low amplitude dynamic load + static drum weight) for the pavement investigated are much smaller in the basecourse and the upper part of the subgrade and at about the same magnitude in the lower part of the subgrade compared with the elastic strains induced by a 40kN loaded dual wheel.

It can be concluded that the compaction effort of a 3t-roller drum at low-amplitude settings seems to be insufficient to apply the required compaction effort on the basecourse to ensure a satisfactory DoC; and hence, to avoid rutting in the basecourse.

Figure 5.8 Vertical elastic strains under a 3t-roller drum and a 40kN loaded dual wheel, 200mm basecourse (DoC 95%); low-amplitude dynamic load + static drum weight

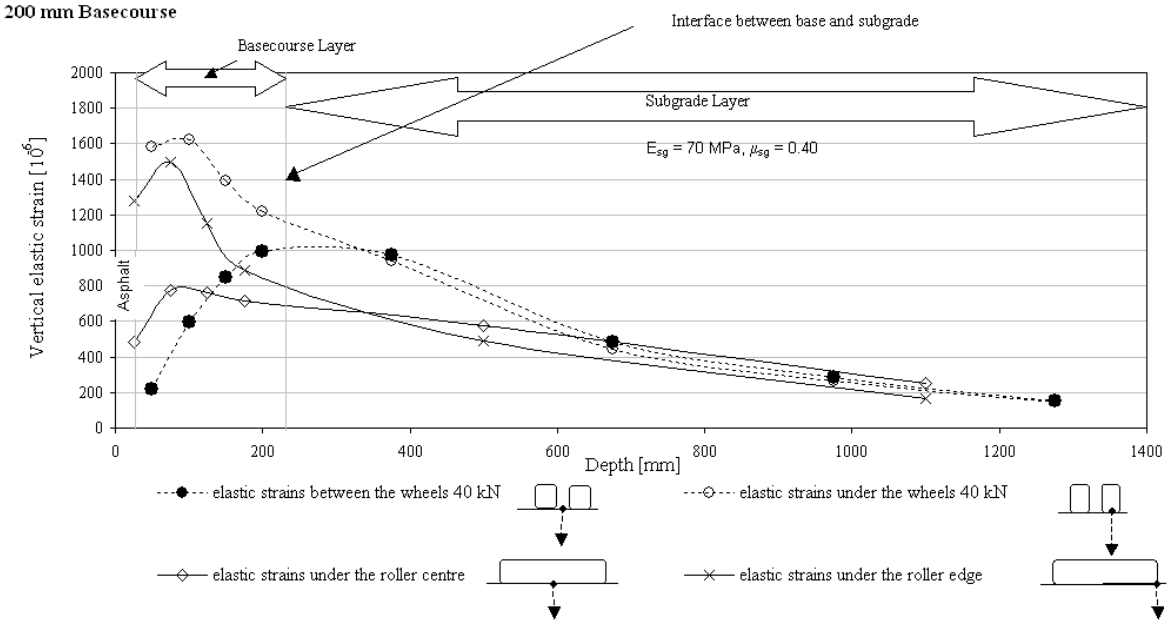

5.4.4 Stress and strains - CAPTIF pavement

Figure 5.9 presents the vertical stress under a 3t-roller drum (high-amplitude dynamic load + static drum weight) and under a 40kN loaded dual wheel of the CAPTIF pavement (PR3-0810 test). Again, the maximum compressive stress under a dual wheel naturally occurs under the middle of the wheel path next to the surface. Figure 5.4 clearly illustrates that the highest vertical stress under a rigid 3t-steel roller drum occurs on the edges. Modifying the elastic modulus of the subgrade (eg from 70MPa to 30MPa for the CAPTIF pavement) does not greatly affect the stress field. However, the effect of a lower subgrade stiffness on the vertical elastic strain pattern under a 3t-roller drum (high-amplitude dynamic load + static drum weight) is more significant and illustrated in figure 5.5.

Figure 5.9 Vertical elastic strains under a 3t-roller drum and a 40kN loaded dual wheel, CAPTIF pavement, (basecourse DoC 95%)

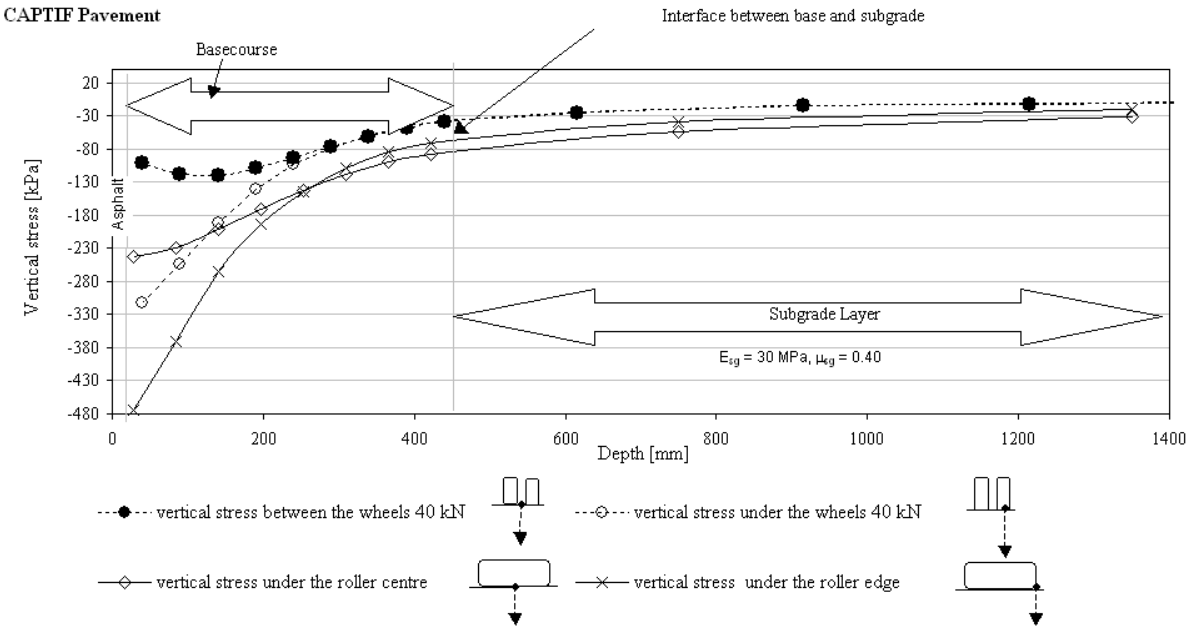

Figure 5.10 Vertical elastic strains under a 3t-roller drum and under a 40kN loaded dual wheel, CAPTIF pavement (basecourse DoC 95%)

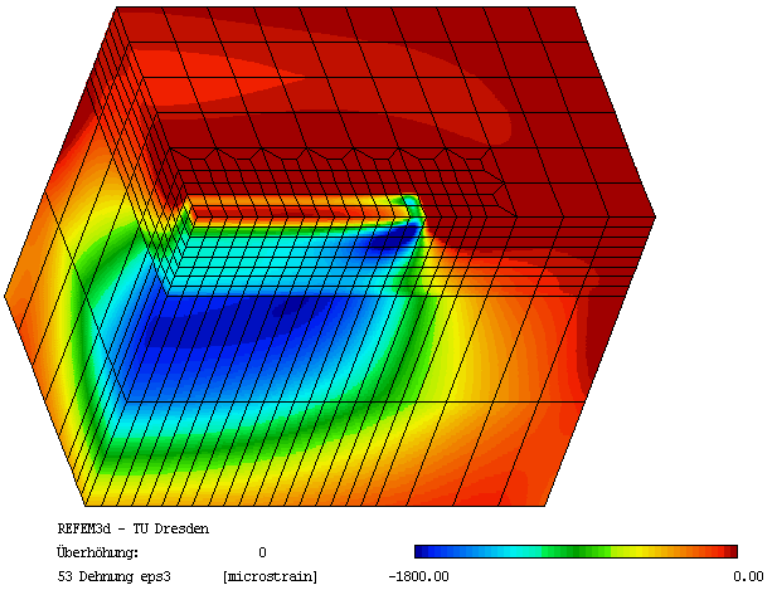

Due to the low subgrade stiffness the highest vertical elastic strains occurring are in the subgrade. Figure 5.11 presents the vertical elastic strains in the basecourse under a 40kN loaded dual wheel and a 3t-roller drum. Again, the vertical elastic strains in the upper part of the basecourse under the 40kN loaded dual wheel are significantly higher compared to the vertical elastic strains induced by a 3t-vibratory roller drum (roller drum centre). Compared with the vertical elastic strains presented in figure 5.11 higher strains in the subgrade and in the lower part of the basecourse occur under a 3t-roller drum due to a lower subgrade stiffness (70 MPa → 30MPa).

Figure 5.11 Vertical elastic strains under a roller and a 40kN loaded dual wheel, CAPTIF pavement, (basecourse DoC 95%)

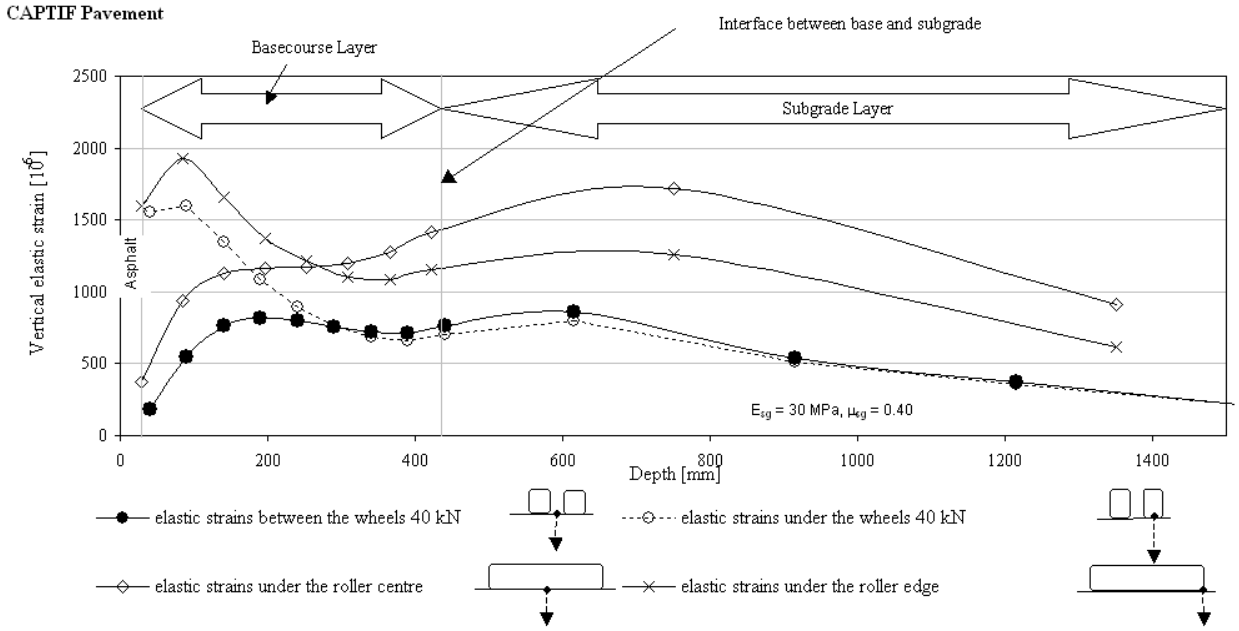

5.4.5 Plastic strains - CAPTIF pavement

This section presents an approach to predict the plastic deformation of the basecourse in pavements using elastic FE calculation results. The investigation is based on RLT test results and uses the axial elastic strain to predict the axial plastic strain rate per load cycle. The relationship is applied to the axial elastic strains calculated earlier and integrated over the depth of the basecourse layer and the number of load cycles in the CAPTIF tests to determine the plastic deformation (rut depth) occurring in the basecourse. Two RLT strain tests were conducted on the basecourse material used at CAPTIF. The material was tested at 95% and 87% DoC and at 70% of OMC.

5.4.5.1 Plastic strain calculation

The raw RLT test data was analysed in terms of elastic axial strain (□el) and the plastic strain rate. Because the initial part of the plastic deformation curve is often influenced by the technique used in preparing the sample, it was decided to focus on the steady state response of the sample (load cycles 20,000 to 50,000).

The elastic strain value (□el) was averaged over the same interval to give an average value of □el. The following exponential relationship between the elastic strain (□el) and plastic strain rate ( ) can be determined.

where: Equation 5.2

	[10-3/cycle]	major principal plastic strain rate
□el	[10-3]	major principal elastic strain
E, F	[-]	material parameter.

Figure 5.12 shows the relationship between axial elastic strain and axial plastic strain rate per load cycle on a (□el) vs. ( ) plot. It can be seen clearly that the lower DoC will result in a higher plastic strain rate at the same magnitude of vertical elastic strains.

Figure 5.12 Axial elastic strain versus plastic strain rate for the Greywacke at 87% and 95% DoC, RLT test results

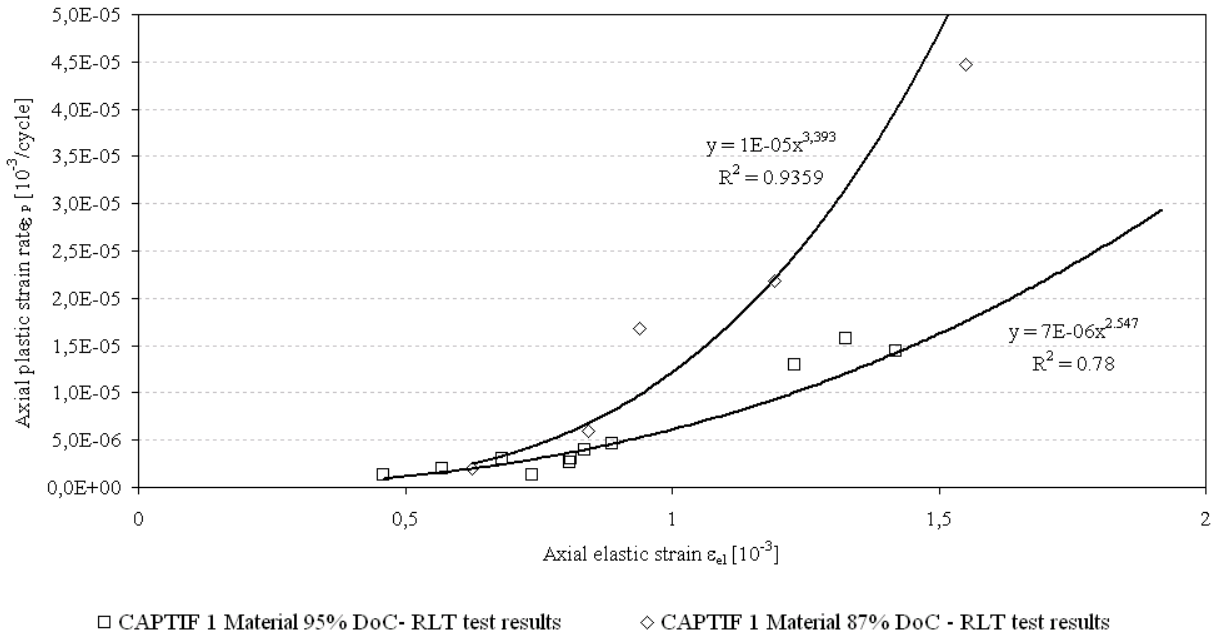

Figure 5.13 illustrates the elastic strain distribution in the basecourse layer under a 40kN wheel load using the FE calculation results. The plastic strain values during the steady state phase were determined for the basecourse using equation 5.2. Figure 5.11 shows that the most critical (maximum) vertical elastic strains and plastic strain rates occur at the top of the basecourse layer (in a depth of 100mm) for the pavement investigated.

Figure 5.13 Elastic and plastic strain rate distribution in the basecourse, CAPTIF pavement; basecourse DoC 87% and 95%

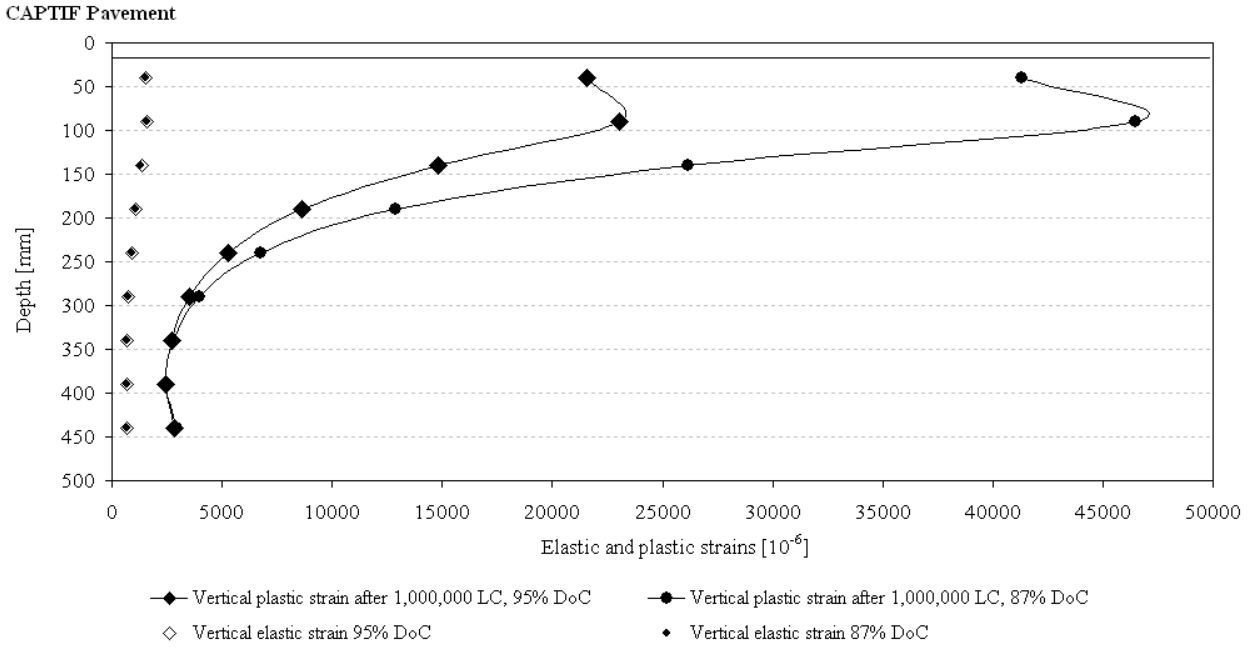

Figure 5.13 clearly demonstrate that the elastic strains in the basecourse due to a 40kN dual wheel load at different DoC of the basecourse are very similar. However, significantly higher plastic strain rates can be observed for the basecourse with a DoC of 87% compared to the basecourse with a DoC of 95%. As from a depth of 300mm the difference between the plastic strain rates are negligible.

5.4.6 Rut depth calculation of the basecourse

The development of plastic deformation at CAPTIF can be divided into the initial post-construction compaction and the steady state phase. The initial post-construction compaction at CAPTIF is usually completed within the first 25,000 to 100,000 load cycles. The amount of plastic deformation that occurred from the start of the test to the completion of post-construction compaction and the plastic deformation that occurred from completion of post-construction compaction to the end of the test were calculated (see table 5.3).

As already explained, the axial elastic strain profile of the pavement was determined for the load applied in the CAPTIF test under the wheels (beneath the centre of one tyre) using FE calculation results. The basecourse layer was divided into a number of sub-layers and the axial elastic strain values at the mid points of the layers were used to determine the value of ( ) for each layer. Finally, the plastic deformation of the basecourse was determined by multiplying each ( ) value by the sub layer thickness and the number of load cycles. The total amount of plastic deformation of the basecourse layer was calculated by summing the contributions of each sub-layer. Tables 5.4 and 5.5 show the magnitudes for the basecourse deformation assuming a compaction level of 88% MDD and 95% MDD for the basecourse at CAPTIF. As expected, the model predicts significantly higher plastic deformation values for the pavement with a basecourse with a DoC of 87% (10.36mm rut depth after one million load cycles) compared to the pavement with a basecourse with a DoC of 95% (7.11mm rut depth after one million load cycles). The results of the calculation clearly demonstrate that is not likely that a lower DoC of the basecourse of 87% would cause a premature failure of the CAPTIF pavement investigated.

Table 5.4 Plastic deformation of the basecourse; CAPTIF pavement, (450mm basecourse – 95% DoC, 40kN load, subgrade stiffness 30MPa)

Depth to midheight of the sub layer	**Sub layer thickness**	**Elastic strains**	**Plastic strain rate steady state**	**Plastic deform-ation steady state**	**Load cycles post-construction compaction**	**Plastic strain rate post-construction compaction**	**Plastic deformation post-construction compaction**
	h		$\dot{\varepsilon}_p$ **=7E-06*$\varepsilon_{el}^{2.547}$**	**v_p= $\dot{\varepsilon}_p$ *h*N**	$N_{pc} = 211.71 \cdot \varepsilon_{el}^{0.8232}$	$\dot{\varepsilon}_{ppc} = 0.0042 \cdot \dot{\varepsilon}_p^{1-0.6869}$	$V_{ppc} = \dot{\varepsilon}_p * h * N$
[mm]	**[mm]**	**[10^{-3}]**	**[10^{-3}/cycle]**	**[mm]**	**[-]**	**[10^{-3}/cycle]**	**[mm]**
440	50	701	2.83E-06	0.14	46595	7.70E-05	0.18
390	50	663	2.46E-06	0.12	44505	7.36E-05	0.16
340	50	688	2.70E-06	0.13	45882	7.58E-05	0.17
290	50	764	3.53E-06	0.17	50015	8.24E-05	0.21
240	50	894	5.26E-06	0.25	56922	9.34E-05	0.27
190	50	1086	8.64E-06	0.40	66809	1.09E-04	0.36
140	50	1342	1.48E-05	0.68	79526	1.29E-04	0.51
90	50	1597	2.31E-05	1.05	91770	1.48E-04	0.68
40	50	1556	2.16E-05	0.98	89826	1.45E-04	0.65
Plastic basecourse deformation after 1 million load cycles [mm]			3.91	3.20	Total deformation 7.1mm		

Table 5.5 Plastic deformation of the basecourse: CAPTIF pavement (450mm basecourse – 87% MDD, 40kN load, subgrade stiffness 30MPa)

Depth to midheight of the sub layer	Sub layer thickness	Elastic strains	Plastic strain rate steady state	Plastic deformation steady state	Load cycles post-construction compaction	Plastic strain rate post-construction compaction	Plastic deformation post-construction compaction
	h		$\dot{\varepsilon}_p$ =1E-05*$\varepsilon_{el}^{3.393}$	$v_p = \dot{\varepsilon}_p * h * N$	$N_{pc} = 211.71 \cdot \varepsilon_{el}^{0.8232}$	$\dot{\varepsilon}_{ppc} = 0.0042 \cdot \dot{\varepsilon}_p^{1-0.6869}$	$V_{ppc} = \dot{\varepsilon}_p * h * N$
[mm]	[mm]	[10^{-3}]	[10^{-3}/cycle]	[mm]	[-]	[10^{-3}/cycle]	[mm]
440	50	699	2.97E-06	0.14	46,485	7.81E-05	0.18
390	50	661	2.45E-06	0.12	44,395	7.36E-05	0.16
340	50	685	2.77E-06	0.13	45,717	7.64E-05	0.17
290	50	761	3.96E-06	0.19	49,854	8.55E-05	0.21
240	50	890	6.73E-06	0.32	56,713	1.01E-04	0.29
190	50	1078	1.29E-05	0.60	66,404	1.24E-04	0.41
140	50	1328	2.62E-05	1.21	78,842	1.54E-04	0.61
90	50	1573	4.65E-05	2.11	90,633	1.85E-04	0.84
40	50	1519	4.13E-05	1.88	88,064	1.78E-04	0.78
Plastic basecourse deformation after 1 million load cycles [mm]			6.70	3.66	Total deformation 10.4mm		

6 Discussion

The CAPTIF test resulted in a rapid failure of a section of the pavement where the lower 150mm of basecourse had been compacted to 87% MDD. Except for this short section there was no significant difference in the rut progression for all the pavements. The density data is confusing in that either there has been a loosening of the basecourse during trafficking or the density measurements are in error. Due to the disturbance of removing the surface a decrease in density was also noted in the field tests performed by Patrick and Alabaster. It is considered that there needs to be further investigations to determine if there is a change in density during traffic loading

The initial change in VDM of 4-6mm up to a 50,000 cycles is typical of results of tests on pavements at CAPTIF (Arnold 2005) and the thickness of the granular layer does not appear to be a significant factor.

There was only rapid failure at two stations in the 88% MDD section. With these two stations removed then the rut progressions to 188,000 cycles are similar. This result is confirmed by the FEM and RLT tests which concluded that the difference between the 88% MDD and 95% MDD was in the order of a few millimetres.

There appears to be no relationship between density and the 'failure'. The areas that failed did not have a density profile significantly different from the rest of the section.

As mentioned above the apparent decrease in density is puzzling. For the VSD a change of 4mm is equivalent to a change in density of the 450mm layer of less than 1%. Even if the 4mm depth is attributed to the top 150mm then the change in density is only 2.5%.

The development of a rut in pavement can be attributed to a consolidation of the layer directly under the wheel and/or shear and heave of the material outside the wheel load.

The VSD plots were examined to see if there was evidence of heave of the materials.

Figures 6.1 and 6.2 show the profiles at 0,2000 and 186000 cycles for stations 25 and 26 where rapid changes occurred. It can be seen that there is no significant heaving of the materials. Therefore it can be concluded that the change in shape is mainly consolidation.

Figure 6.1 Change in profile with loading at station 25

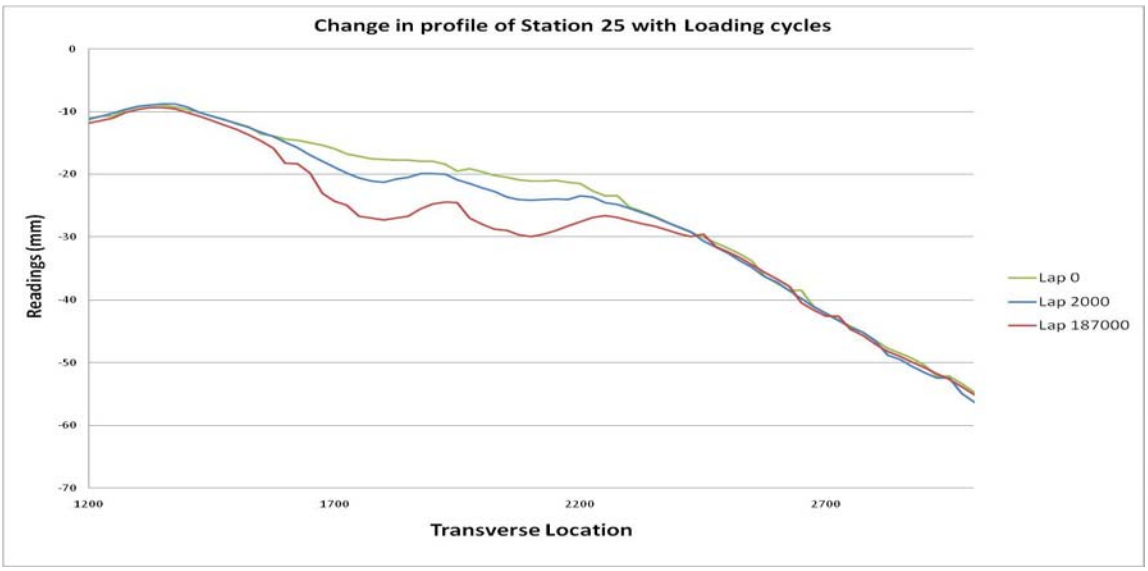

Figure 6.2 Change in profile with loading at station 26

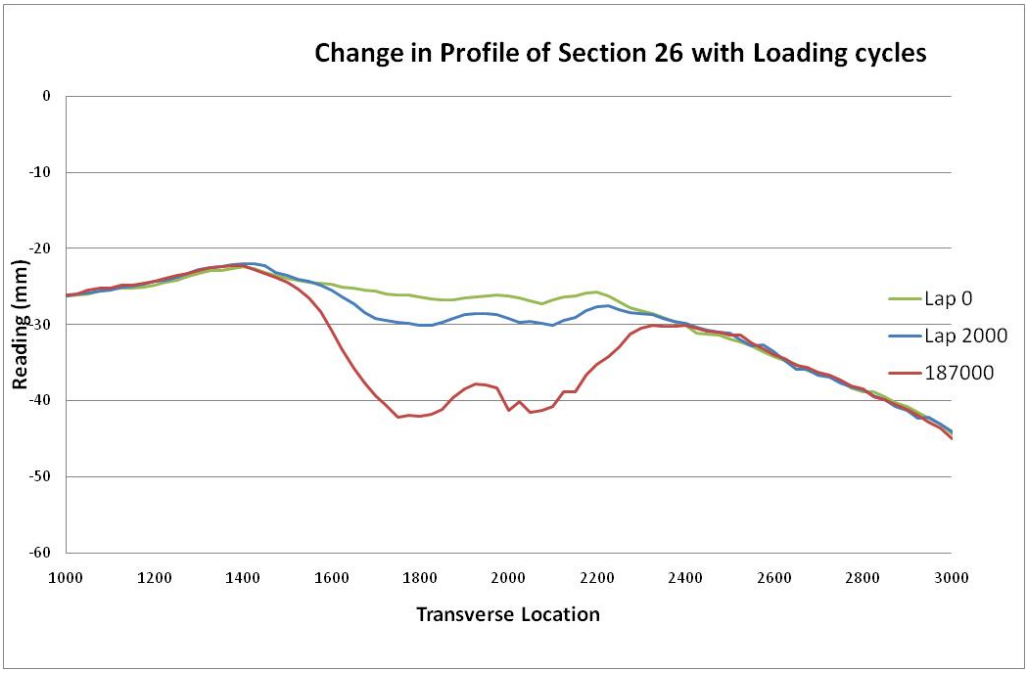

The FEM has shown that the stress conditions near the top of the basecourse under the vibratory roller are lower than those under the standard wheel load. This suggests that the build up of residual stresses in the pavement under the roller may not be the same as those generated under the wheel load. The significance of residual stresses in influencing the strength of a granular pavement has been noted by Arnold (2004).

None of the above assists in determining the absolute reasons for the premature failure of some thick granular pavements which prompted this research project.

It could be postulated that the failure of these pavements in the field is not associated with the thickness of granular material but rather that these pavements have been on high traffic volume roads and that the initial consolidation of 5–8mm is enough to allow the development of a film of water in wet conditions.

Under the action of traffic the water is pushed through the seal resulting in premature shear failure. The phenomena of water being pushed through a first-coat seal has been reported by Patrick (2009) and is the subject of current testing at CAPTIF.

7 Conclusions

The conclusion of the research is that in using conventional New Zealand construction techniques and specifications some post-construction deformation of greenfield pavements appears to be inevitable. The permanent strain developed will manifest itself into a larger rut depth as the granular thickness increases. However, the rut depth should not approach the levels (20mm) that prompted the initiation of this research.

This research has demonstrated that the initial post-construction deformation of a thin-surfaced granular pavement is affected by the compaction level achieved in the field although the depth of the rut would be relatively small. It has also demonstrated that there is probably a contribution from the compaction equipment used.

The results of the RLT testing and FEM modelling support the above conclusions in that a degree of compaction of 88% MDD would not result in significant rutting in the pavement. The testing and modelling suggested that after one million load applications the difference in rut depth of a granular layer of 450mm depth that had been compacted to 88% MDD and one that had been compacted to 95% MDD would be approximately 3mm.

The results of the FE calculations indicate that the maximum vertical elastic strains and vertical compressive stress induced by a 3t-roller drum (high-amplitude dynamic load + static drum weight) in the upper part of the basecourse are smaller than the stresses and elastic strains induced by a 40kN dual wheel for the pavements investigated. The vertical compressive stress and elastic strains induced by a 3t-roller drum at the lower part of the basecourse are considerably higher than the stress and strains induced by a 40kN loaded dual wheel for the pavements investigated.

It would appear that as the compaction system does not build up residual stresses in the pavement, when traffic loading does occur granular material is moved in such a way that there is a build up of those stresses that can resist the wheel loading.

It is postulated that the shear deformation found in the field is associated not just with post-construction rutting but is exacerbated by water being forced through the surface by vehicle tyres.

Research into the influence of the compaction methodology and the waterproofing ability of thin surfacings on the performance of unbound granular materials is continuing.

8 References

Arnold, G (2004) Investigation into aggregate shakedown and its influence on pavement performance. PhD thesis, University of Nottingham, UK.

Arnold, G, B Steven, D Alabaster and A Fussell (2005) Effect on pavement wear of increased mass limits for heavy vehicles. Concluding report. *Land Transport NZ research report no.281*.

New Zealand Standard NZS 4402 Test 4.1.3 Determination of the dry density/water content relationship, NZ vibrating hammer test.

Oeser, M (nd) Numeric simulation of the non-linear behaviour of flexible pavements (in German: Numerische Simulation des nichtlinearen Verhaltens flexibler mehrschichtiger Verkehrswegebefestigungen), PhD thesis, University of Technology, Dresden, Germany.

Patrick, JE and DJ Alabaster (1998) Pavement density. *Transfund NZ research report no.100*.

Pidwerbesky, BD (1995) Accelerated dynamic loading of flexible pavements at the Canterbury accelerated pavement testing indoor facility. *Transportation research record 1482*. pp79–86.

Sandström, A (1994) Numerical simulation of a vibratory roller on cohesive soil. *Geodynamic research report 2007*.

Ping Yang, Z, M Leonhard and S Puchta (2002) Laboratory Simulation of Field Compaction characteristics on sandy soils, *Transportation research record 1808*, paper no. 02–3164.

Transit New Zealand (2005) *Specification for construction of unbound granular pavement, TNZ B/2:2005.*

Transit New Zealand (2006*) Specification for base-course aggregate, TNZ M/04.*

Werkmeister, S (2003) Permanent deformation behaviour of unbound granular materials. PhD thesis, University of Technology, Dresden, Germany.

Werkmeister, S, BD Steven, DJ Alabaster, G Arnold and M Oeser (2005) 3D finite element analysis of accelerated pavement test results from New Zealand's CAPTIF facility, bearing capacity of roads, railways and airfields: *Proceedings of the 7th International Symposium on the Bearing Capacity of Roads and Airfields (BCRA), Trondheim* (N), June 2005.